ELSEVIER

Journal of Alloys and Compounds 300–301 (2000) 275–282

Journal of ALLOYS AND COMPOUNDS

www.elsevier.com/locate/jallcom

Spectroscopy and structure of Eu(III) complex with *N*-methylglycine

Paula P. Gawryszewska, Lucjan Jerzykiewicz, Piotr Sobota, Janina Legendziewicz*

Faculty of Chemistry, University of Wroclaw, 14 F. Joliot-Curie Str., 50-383 Wroclaw, Poland

Abstract

Synthesis and spectroscopic characterization of a Eu(III) complex with *N*-methylglycine (sarcosine=sar) are reported. The crystal structure was determined by X-ray diffraction with the final $R=0.036$. The compound crystallizes in the *P1* space group with $Z=1$. In the structure dimeric units are formed in which two metal ions are linked by four carboxyl groups; two simple bridging and two chelating ones. The $[Eu(C_3O_2H_7N)_3(H_2O)_2]_2^{6+}$ dimeric cationic units are further linked by two simple carboxyl bridges forming a polymeric chain. In the dimeric cation the lanthanide ions occupy two nonequivalent structure positions. Amino acid molecules reside as zwitterions; thus nitrogen atoms are not involved in metal ion coordination. Absorption, emission and excitation spectra down to 4 K are reported. The number of Stark components is determined from low temperature spectra, and the symmetry of metal centers is described. The effect of the polymeric structure on spectroscopic properties is discussed. Electron–phonon coupling is considered and vibronic components are assigned based on IR and Raman data. Their intensities are related to the theory of vibronic transition probabilities. The electron transition probabilities are analyzed and the temperature dependence of the oscillator strength values are considered.

Keywords: Sarcosine; Europium; X-ray; Spectroscopy; Cooperative interaction; Vibronic coupling

1. Introduction

The studies of structure and optical properties of dimeric and polymeric lanthanide compounds have received considerable attention in recent years. On the one hand, they may show up-conversion properties and thus may be applied as potential laser materials [1]; on the other hand, effectiveness of some biologically significant processes, such as energy transfer and electron transfer, depend on the structure and dimensionality of polymeric chains [2–6]. A one-dimensional system imposes the highest restriction on ion–ion interaction, and energy migration that depends on such interactions between nearest neighbor in the lattice will thus be dominant in the chain direction. Research studies on polynuclear lanthanide compounds may contribute to providing information concerning exchange and magnetic interaction mechanisms [7–10].

The f–f electron transitions of the rare earth ions are accompanied by (usually) weak vibronic transitions. Because their intensity yields information on the coupling of the $4f^n$ electron to the surroundings, they are intensively investigated [11–14]. Thus vibronic coupling can be used as a test of the coordination mode of ligand molecules, especially in complex biologically important systems.

In our previous papers the spectroscopic and X-ray data for lanthanide complexes with α,β-alanine, isoleucine and glycine (α,β-Ala, Ile, Gly) [15–20] and their aminohydroxamic analogues (α-Alaha, β-Alaha) [21,22] were reported. The influence of ligand chirality on the structure and spectroscopic properties of dimeric and polymeric rare earth compounds were analyzed [23,24]. It is worth noting that dimers are created in crystal structures for light lanthanides in the majority of complexes with monocarboxylic amino acids.

The goal of the present study is synthesis and X-ray characterization of a 1:3 europium complex with sarcosine. In addition, the results concerning the influence of the polymeric structure of the Eu(III) complex with methylglycine (sarcosine=sar) on its spectroscopic properties, are presented. The vibronic coupling is analyzed and related to the chemical constitution of lanthanide ion surroundings.

2. Experimental

Single crystals of $[Eusar_3(H_2O)_2](ClO_4)_3.H_2O$ (further denoted as Eu:sar) were obtained by slow evaporation of a

*Corresponding author. Tel.: +48-71-320-4300; fax: +48-71-328-2348.

E-mail address: jl@wchuwr.chem.uni.wroc.pl (J. Legendziewicz)

0925-8388/00/$ – see front matter
PII: S0925-8388(99)00721-5

Table 1
Crystal data and structure refinement for $[Eu(sar)_3(H_2O)_2](ClO_4)_3.H_2O$[a,b]

Empirical formula	C18 H30 Cl6 Eu2 N6 O42
Formula weight	1519.1
Temperature	299(2) K
Wavelength	0.71073 Å
Crystal system	Triclinic
Space group	*P1*
Unit cell dimensions	$a=9.146(2)$ Å, $\alpha=100.42(3)$ deg.
	$b=11.042(2)$ Å, $\beta=104.56(3)$ deg.
	$c=14.696(3)$ Å, $\gamma=109.24(3)$ deg.
Volume	1298.6(5) $Å^3$
Z	1
Density (calculated)	1.943 Mg/m^3
Absorption coefficient	2.817 mm^{-1}
F(000)	744
Crystal size	0.8×0.5×0.4 mm
Theta range for data collection	2.04 to 28.07 deg.
Index ranges	$0\le h\le 10,\ -13\le k\le 13,\ -18\le l\le 18$
Reflections collected	5876
Independent reflections	5875 [R(int)=0.0318]
Absorption correction	Difabs procedure
Max. and min. absorption	1.26 and 0.92
Refinement method	Full-matrix least-squares on F^2
Data/parameters	5875/547
Goodness-of-fit on F^2	1.086
Final R indices [$I>2\sigma(I)$]	$R_1=0.0366$, $wR_2=0.1011$
R indices (all data)	$R_1=0.0377$, $wR_2=0.1023$
Largest diff. peak and hole	1.218 and −1.378 e. $Å^{-3}$

[a] $R_1=\Sigma(F_o-F_c)/\Sigma F_o$.
[b] $wR_2=\{\Sigma[w(F_o^2-F_c^2)^2]/\Sigma[w(F_o^2)^2]\}^{1/2}$.

solution with a 1:1 $Eu(ClO_4)_3$:ligand molar ratio, pH=4.5 at room temperature. The chemical composition was checked by elemental analysis, and the Eu(III) content by the ICP-AES method.

The crystals were sealed in glass capillaries under a nitrogen stream. Preliminary examination and intensity data collections were carried out on a KUMA KM-4 four-circle diffractometer [25] using graphite-monochromated Mo-Kα radiation. The recorded data were corrected for Lorentz and polarization factors. In addition, absorption correction following the DIFABS [26] procedure was applied. The crystal data and some features of the structure refinement are summarized in Table 1. The structures were solved by direct methods (SHELXS97) [27] and refined on F^2 by full-matrix least-squares program (SHELXL93) [28]. The carbon bonded H-atoms were included in the calculated positions and refined using a riding model with isotropic displacement parameters equal to 1.2 U_{eq} of the attached C atom. Because of disorder the H atoms of water molecules were not localized. All the atoms of ClO_4^- anions were found disordered.

Absorption, emission and excitation spectra were measured in the 293 to 4 K temperature range. Low temperature spectra were recorded using a CF 1204 Oxford helium flow cryostat, the absorption on a Cary-Varian 5 spectrophotometer, the emission and excitation on an SLM AMINCO SPF-500 spectrofluorometer equipped with a 300 W xenon lamp. IR and Raman spectra at 293 K were measured on a Brücer FS88 FTIR and on a FTIR NICOLET MAGNA 860 with Raman equipment using a Nd laser.

3. Results and discussion

The $[Eusar_3(H_2O)_2](ClO_4)_3.H_2O$ complex crystallizes in a triclinic system and *P1* space group. In the structure, the sarcosine molecules are zwitterions. The Eu:sar complex is a linear polymer built of dimeric units with two non-equivalent Eu(III) ion positions (Fig. 1). The coordi-

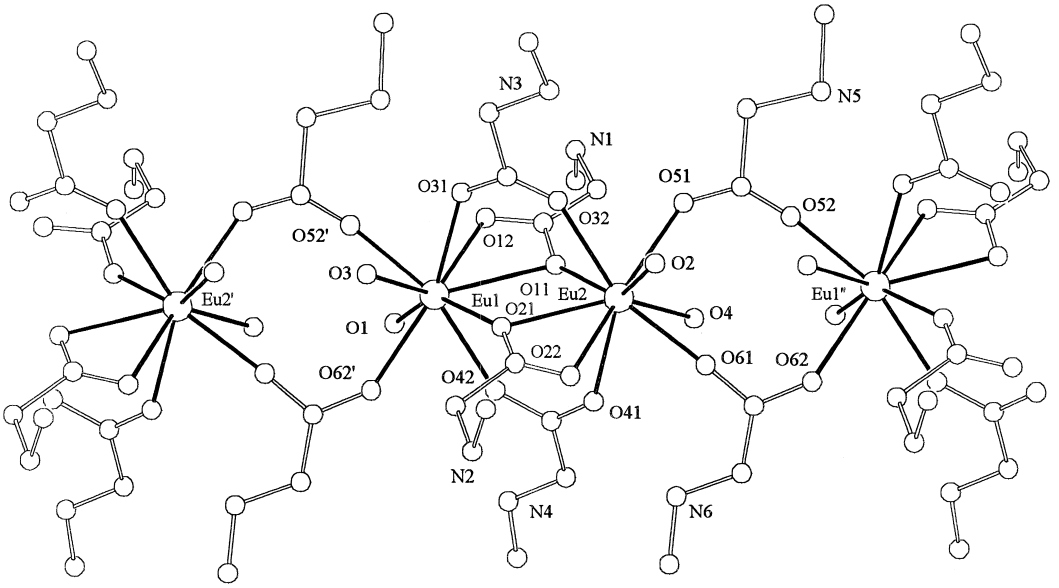

Fig. 1. The structure of the polymer $[Eu(sar)_3(H_2O)_2](ClO_4)_3.H_2O$.

nation number (CN) of Ln(III) ion is equal to 9, and the kind of coordination mode of the carboxylic groups corresponds to those in lanthanide complexes with glycine [19,20]. Note that the composition of the europium compounds presented corresponds to those for heavy lanthanides. $[Eusar_3(H_2O)_2]_2^{6+}$ dimer cations are linked by two simple carboxylic bridges forming an endless polymer. Eu(III) ions in dimers are bonded by four carboxylic bridges of four sarcosine molecules. Two of them include type I (Asłanow [29]) carboxylic group coordination, a double-bond bridge; the next two have a three-bond cyclic-bridge carboxylic group (type II coordination). Each Eu(III) ion is coordinated by seven oxygen atoms of six sarcosine molecules and two oxygen atoms of water. The outer coordination sphere is comprised of six ClO_4^- ions and two water molecules. M–M distances within the Eu:sar structure are as follows: Eu1–Eu2=4.015 Å, Eu1–Eu2′=5.240 Å and Eu2–Eu1″=5.240 Å and are shorter than in Nd(III), Ho(III) and Dy(III) compounds with glycine. Average bond Ln1–O and Ln2–O lengths in Eu:sar are almost the same as in $Ho_2(Gly)_6(ClO_4)_6(H_2O)_6$ (Ho1–O=2.452 Å, Ho2–O=2.442 Å) and in $Nd_2(Gly)_6(ClO_4)_6 9H_2O$ (Nd1–O=2.529 Å, Nd2–O=2.512 Å); they are, respectively, 2.456 Å and 2.452 Å (Table 2). Eu1–O12 (2.607 Å) is the longest bond in the Eu(III) compound with sarcosine, where O12 is an oxygen atom of the three-bond cyclic bridge carboxylic group and is linked with only one lanthanide ion. The Eu2–O22 bond with a monodentate oxygen atom of a different three-bond cyclic bridge carboxylic group, is also one of the longest (2.563 Å), and is comparable with bond lengths of Eu2–O2(H_2O)=2.495 Å, Eu2–O4(H_2O)=2.599 Å. M–O bonds in lanthanide:glycine complexes are the longest, where an oxygen atom also originates from the three-bond cyclic bridge carboxylic group, but it is linked with two lanthanide ions (Ho1–O11=3.152 Å; Ho2–O14=3.116 Å; Nd1–O12=3.037 Å; Nd2–O25=2.773 Å); their length is larger than between a lanthanide ion and the oxygen atoms of a water molecule. Some selected bond lengths and angles are provided in Table 2.

The ninefold coordination of the metal in the complexes can form two types of ideal coordinate polyhedra; a tricapped trigonal prism TCTP (symmetry D_{3h}) or a capped square antiprism CSAP (symmetry C_{4v}). In reality, nine-coordinate lanthanides often have an intermediate geometry between the two ideal polyhedra. Transitions from one ideal coordinate polyhedra to another can take place through various symmetries of a coordinating object. Matching of coordinate polyhedra, according to Drew [30], for the Eu(1) and Eu(2) sites in Eu:sar, as shown by crystallographic measurements, points to a symmetry closer to C_{4v}, though the Δ deviation parameter is high for both CSAP and TCTP, and equals, respectively, Eu1 $\Delta_{CSAP}=0.08365$ Å^2, $\Delta_{TCTP}=0.12485$ Å^2; Eu2 $\Delta_{CSAP}=0.06527$ Å^2, $\Delta_{TCTP}=0.10926$ Å^2. Therefore it seems that a coordinate polyhedra is a middle stage between the two,

Table 2
Selected geometrical parameters (Å) for $[Eu(sar)_3(H_2O)_2](ClO_4)_3.H_2O$

Eu(1)–O(31)	2.387(12)
Eu(1)–O(21)	2.394(12)
Eu(1)–O(42)	2.425(13)
Eu(1)–O(3)	2.466(12)
Eu(1)–O(1)	2.563(12)
Eu(1)–O(11)	2.581(11)
Eu(1)–O(12)	2.607(12)
Eu(1)–Eu(2)	4.0148(11)
Eu(2)–O(11)	2.305(10)
Eu(2)–O(61)	2.346(12)
Eu(2)–O(51)	2.362(12)
Eu(2)–O(41)	2.445(11)
Eu(2)–O(32)	2.446(10)
Eu(2)–O(2)	2.495(12)
Eu(2)–O(21)	2.508(10)
Eu(2)–O(22)	2.563(11)
Eu(2)–O(4)	2.599(12)
O(31)–Eu(1)–O(21)	75.8(4)
O(31)–Eu(1)–O(42)	134.9(4)
O(21)–Eu(1)–O(42)	74.0(4)
O(31)–Eu(1)–O(3)	67.7(4)
O(21)–Eu(1)–O(3)	74.9(4)
O(42)–Eu(1)–O(3)	132.5(4)
O(31)–Eu(1)–O(1)	133.1(4)
O(21)–Eu(1)–O(1)	146.2(4)
O(42)–Eu(1)–O(1)	72.3(4)
O(3)–Eu(1)–O(1)	127.6(4)
O(31)–Eu(1)–O(11)	69.2(4)
O(21)–Eu(1)–O(11)	68.5(3)
O(42)–Eu(1)–O(11)	69.0(4)
O(3)–Eu(1)–O(11)	128.6(4)
O(1)–Eu(1)–O(11)	102.2(4)
O(31)–Eu(1)–O(12)	72.9(4)
O(21)–Eu(1)–O(12)	118.0(4)
O(42)–Eu(1)–O(12)	92.9(4)
O(3)–Eu(1)–O(12)	133.6(4)
O(1)–Eu(1)–O(12)	67.7(4)
O(11)–Eu(1)–O(12)	50.7(3)
O(11)–Eu(2)–O(61)	145.0(4)
O(11)–Eu(2)–O(51)	86.6(4)
O(61)–Eu(2)–O(51)	95.7(5)
O(11)–Eu(2)–O(41)	76.5(4)
O(61)–Eu(2)–O(41)	78.1(4)
O(51)–Eu(2)–O(41)	136.6(4)
O(11)–Eu(2)–O(32)	74.7(3)
O(61)–Eu(2)–O(32)	139.2(4)
O(51)–Eu(2)–O(32)	72.4(4)
O(41)–Eu(2)–O(32)	136.9(4)
O(11)–Eu(2)–O(2)	143.0(4)
O(61)–Eu(2)–O(2)	70.5(4)
O(51)–Eu(2)–O(2)	77.1(4)
O(41)–Eu(2)–O(2)	136.5(4)
O(32)–Eu(2)–O(2)	68.9(4)
O(11)–Eu(2)–O(21)	71.1(3)
O(61)–Eu(2)–O(21)	122.1(4)
O(51)–Eu(2)–O(21)	139.4(4)
O(41)–Eu(2)–O(21)	71.7(4)
O(32)–Eu(2)–O(21)	69.1(4)
O(2)–Eu(2)–O(21)	100.4(4)
O(11)–Eu(2)–O(22)	119.5(4)
O(61)–Eu(2)–O(22)	74.4(4)
O(51)–Eu(2)–O(22)	147.1(4)

Table 2. Continued

O(41)–Eu(2)–O(22)	73.1(4)
O(32)–Eu(2)–O(22)	94.5(4)
O(2)–Eu(2)–O(22)	70.1(4)
O(21)–Eu(2)–O(22)	50.1(3)
O(11)–Eu(2)–O(4)	76.4(4)
O(61)–Eu(2)–O(4)	71.8(4)
O(51)–Eu(2)–O(4)	69.9(4)
O(41)–Eu(2)–O(4)	67.3(4)
O(32)–Eu(2)–O(4)	133.2(4)
O(2)–Eu(2)–O(4)	126.1(4)
O(21)–Eu(2)–O(4)	132.3(4)
O(22)–Eu(2)–O(4)	132.0(4)
Eu(1)–O(21)–Eu(2)	110.0(4)

and the symmetry is defined by transformation of one structure into the other. The spectroscopic studies also seem to confirm these findings.

Luminescence and excitation spectra of the $[Eu(C_3O_2H_7N)_3(H_2O)_2](ClO_4)_3.H_2O$ compound show a higher symmetry of the surroundings of the europium ion in the structure, as compared with other lanthanide compounds with amino acids (Figs. 2a,b and 3). It is apparent by the very low intensity of 0–0 transition, and by the relative ratios of the transition intensities $^5D_0 \rightarrow {}^7F_2$ / $^5D_0 \rightarrow {}^7F_1$ and $^7F_0 \rightarrow {}^5D_2$ / $^7F_0 \rightarrow {}^5D_1$ at 200 K and 4 K temperature (Figs. 2a,b and 3), which are much lower for sarcosine compounds, as compared with europium com-

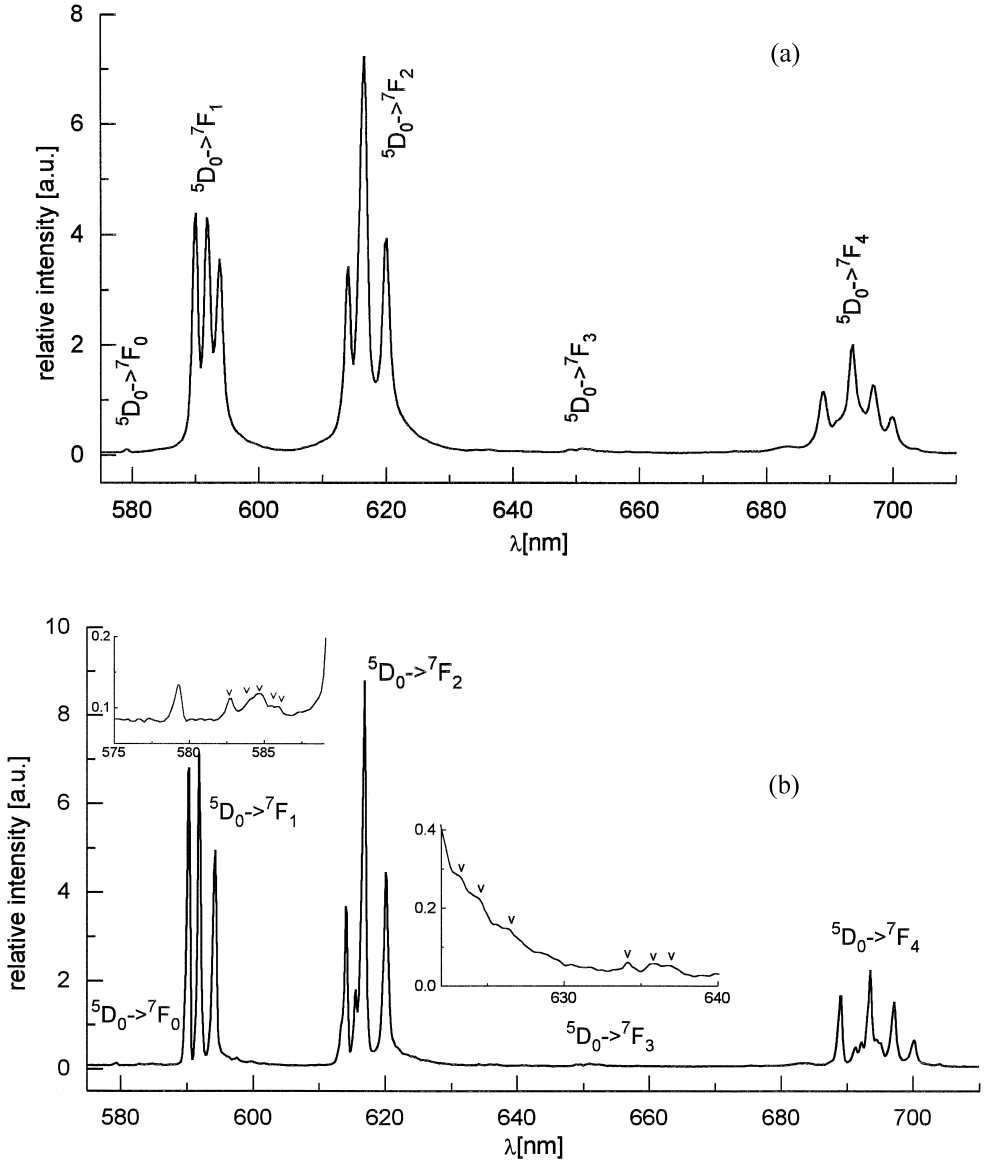

Fig. 2. Luminescence spectra of $[Eu(sar)_3(H_2O)_2](ClO_4)_3.H_2O$ at 200 K (a) and 4 K (b).

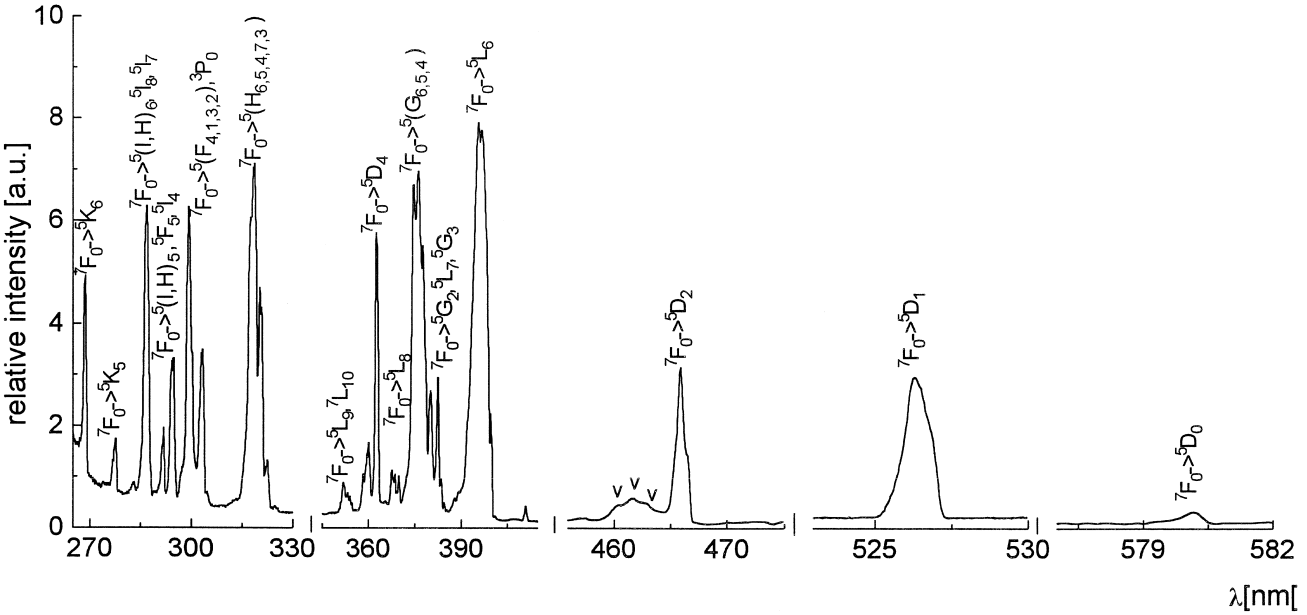

Fig. 3. Excitation spectrum of $[Eu_1(sar)_3(H_2O)_2](ClO_4)_3.H_2O$ at 4 K.

pounds with α-alanine, isoleucine and α-alaninehydroxamic acid [15–18,21,22].

The $^5D_0 \rightarrow {}^7F_2$ transition shows a doublet (of different intensities) structure of three lines resulting from two non-equivalent positions of europium ions in the structure of Eu:sar (Fig. 4). Due to the very low intensity of 0–0 transition, luminescence measurement in this area of the spectrum was performed with the device set to lower resolution, and so the respective band for the $^5D_0 \rightarrow {}^7F_0$ transition at 4 K temperature, is a singlet with a 14 cm^{-1} half width (Fig. 4a), which suggests existence of two non-equivalent positions of lanthanide ions in the structure. In the absorption spectrum, the $^7F_0 \rightarrow {}^5D_0$ band is undetectable; it would be necessary to have a 0.5-cm-thick crystal to make the measurement. Other transitions ($^7F_0 \rightarrow {}^5D_{1,2}$), however, show splitting of individual lines. It is the relatively small splitting (in $^7F_0 \rightarrow {}^5D_2$ transition ~5 cm^{-1}), which suggests a slight structure disordering of

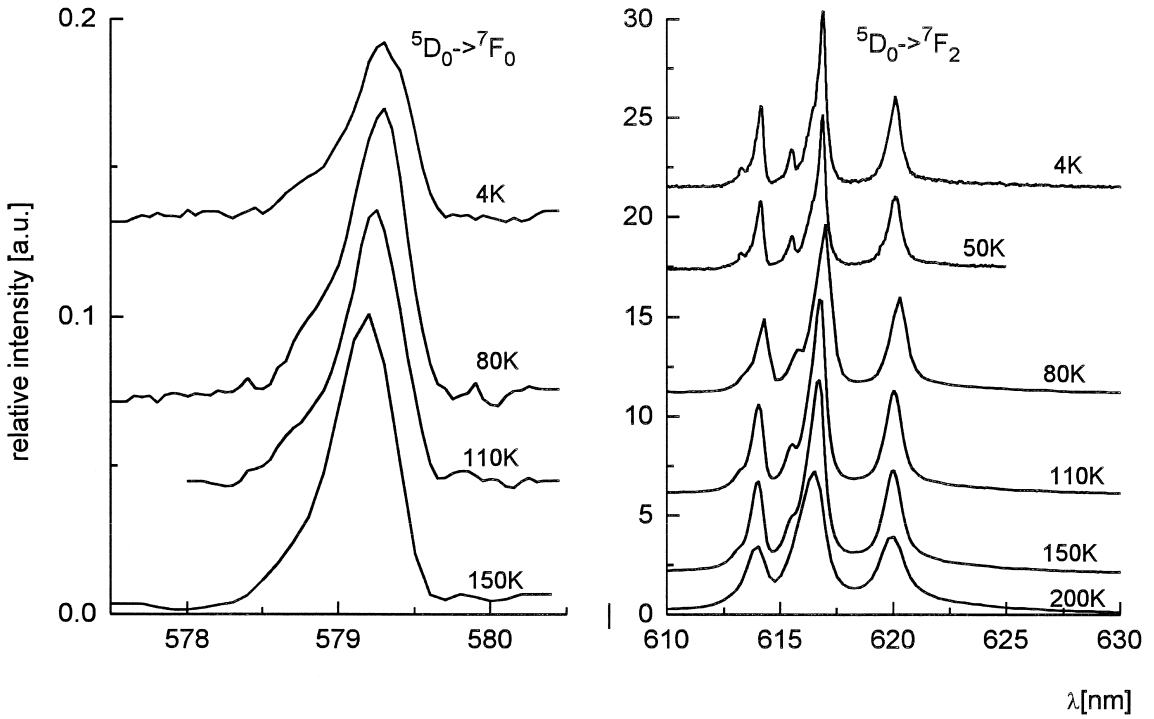

Fig. 4. Luminescence temperature dependence of (a) $^5D_0 \rightarrow {}^7F_0$, (b) $^5D_0 \rightarrow {}^7F_2$ transitions.

the respective europium centers in the dimer (Fig. 4b). As the temperature is lowered from 200 K to 4 K, some differences in relative ratios of $^5D_0 \rightarrow {}^7F_2 / {}^5D_0 \rightarrow {}^7F_1$ transition intensity can be observed. On this basis one could suppose a small transformation of the structure.

Based on group theory considerations and the 4 K luminescence spectrum, a symmetry of the europium ion surrounding was defined as D_2. For this symmetry, the $^5D_0 \rightarrow {}^7F_0$ transition is forbidden due to the selection rules of both magnetic and electric dipole, whereas in $^5D_0 \rightarrow {}^7F_J$ (where $J = 1, 2, 4$) transitions, 3, 3 and 6 components in D_2 symmetry should be observed. In fact, in the spectra investigated such was the number of components recorded at 4 K.

Similarly to the alanine and isoleucine compounds, identification of f–f transitions of the europium ion was carried out in the visible and ultraviolet spectra, up to 280 nm at 293 K and 4 K (Fig. 5). The ultraviolet region also includes results from the excitation spectrum at 4 K (Fig. 3). A significant difference can be observed in relative intensity ratios of europium ion f–f transitions within 280 to 380 nm, as compared with other, previously studied,

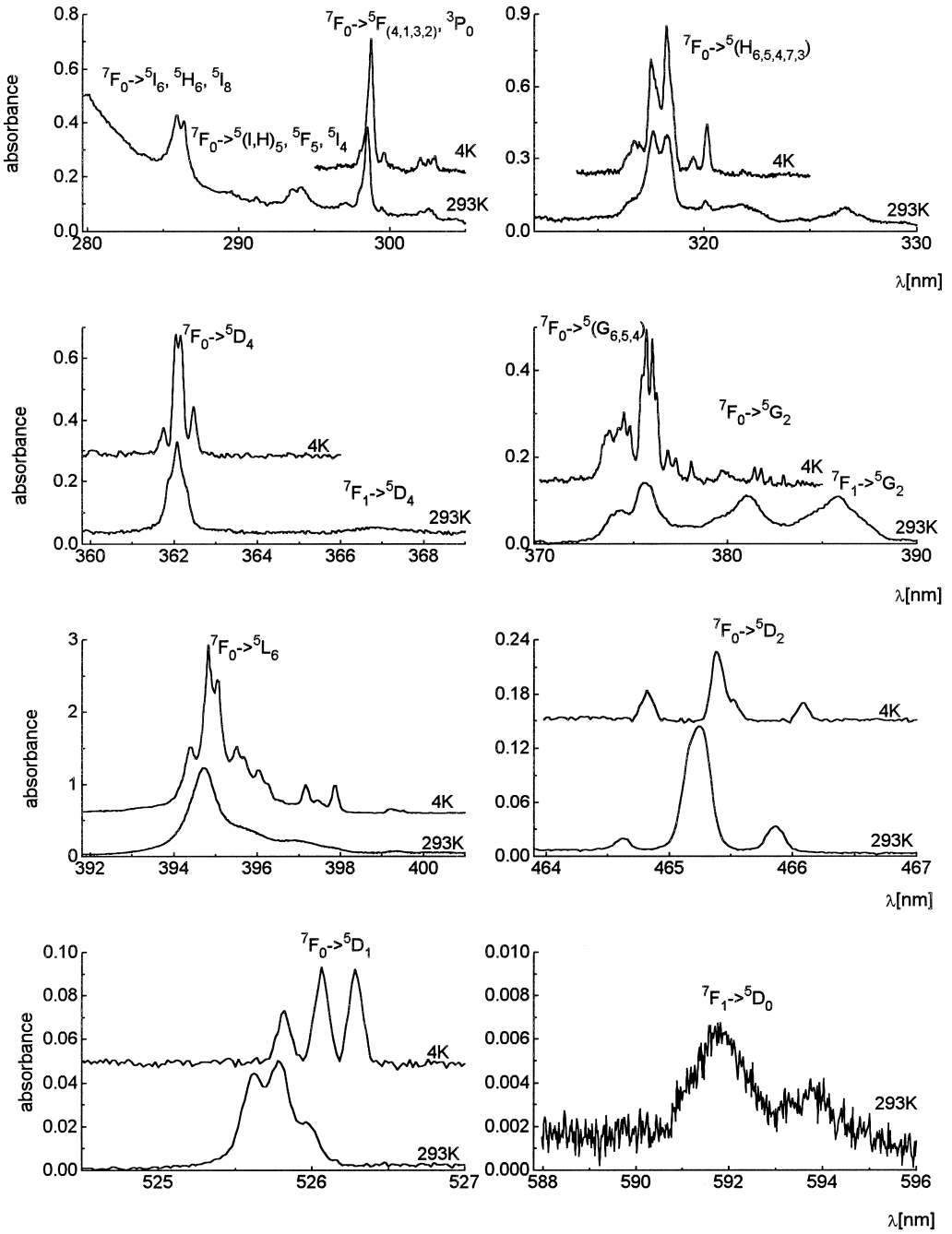

Fig. 5. Absorption spectra of $[Eu(sar)_3(H_2O)_2](ClO_4)_3.H_2O$ at 293 K and 4 K.

Table 3
The oscillator strength values of $[Eu(sar)_3(H_2O)_2](ClO_4)_3.H_2O$[a]

Range	$S'L'J'$	$P \times 10^8$		
		293 K		4 K
		P_{exp}	P_{cal}	
5890–5980	$^7F_1 \rightarrow {}^5D_0$	1.04		
5789–5801	$^7F_0 \rightarrow {}^5D_0$	≈0.04		
5333–5390	$^7F_1 \rightarrow {}^5D_1$	1.07	Z^*[b]	
5240–5270	$^7F_0 \rightarrow {}^5D_1$	1.43		0.90
4640–4670	$^7F_0 \rightarrow {}^5D_2$	3.84	Z^*[b]	1.48
4130–4202	$^7F_1 \rightarrow {}^5D_3$	3.68	32.14	
3900–4070	$^7F_0 \rightarrow {}^5L_6$	251.00	270.21	290.24
3832–3902	$^7F_1 \rightarrow {}^5G_2$	43.94	31.24	
3782–3832	$^7F_0 \rightarrow {}^5G_2$	43.36	31.64	
3707–3782	$^7F_0 \rightarrow {}^5G_4, {}^5G_5, {}^5G_6$	51.52	77.87	79.30
3645–3688	$^7F_1 \rightarrow {}^5D_4$	4.15	8.51	
3601–3645	$^7F_0 \rightarrow {}^5D_4$	22.90	13.55	21.93
3140–3301	$^3F_0 \rightarrow {}^5H_3, {}^5H_7, {}^5H_4, {}^5H_5$	189.12	139.33	141.34
2957–3090	$^7F_0 \rightarrow {}^5(F_{4,1,3,2}), {}^3P_0$	69.62	77.74	69.42
2907–2957	$^7F_0 \rightarrow {}^5(I,H)_5, {}^5F_5, {}^5I_4$	28.78		
2840–2880	$^7F_0 \rightarrow {}^5(I,H)_6, {}^5I_8$	65.18	40.91	64.08

[a] $\tau_2 \times 10^9 = 20.09 \pm 11.68$, $\tau_4 \times 10^9 = 4.46 \pm 2.49$, $\tau_6 \times 10^9 = 6.88 \pm 0.63$.
[b] Z^* transitions which were not taken for calculations.

europium amino acid compounds. Europium ion f–f transitions within 280 to 380 nm in the excitation spectrum of Eu:sar compound at 4 K, have intensities similar to that of the $^7F_0 \rightarrow {}^5L_6$ transition. The oscillator strength values for lines recorded in $[Eu_1(C_3O_2H_7N)_3(H_2O)_2](ClO_4)_3.H_2O$ spectra are much lower than in the case of the alanine and isoleucine compounds with europium; it is mostly related to the hypersensitive transition (Table 3). The difference results from higher symmetry of the lanthanide ion surrounding. The same table includes the Judd–Ofelt [31,32] parameter values calculated according to the procedure described in Ref. [33]. The Judd parameters are evaluated with relatively low errors of estimation. The values of these parameters differ from those for aqua ions and are drastically higher in comparison to other lanthanide carboxylate systems [34].

As the temperature is lowered, the oscillator strength values decrease for most transitions, $^7F_0 \rightarrow {}^5D_2$ and $^7F_0 \rightarrow {}^5D_1$ among others. A slight increase in the intensity can be observed solely for the $^7F_0 \rightarrow {}^5L_6$ transition. A decrease of the oscillator strength values for f–f transitions of europium ion may result from the contribution of a vibronic mechanism in the intensity of f–f transitions, or a slight change in the structure at low temperature.

Luminescence and excitation spectra of $[Eu(C_3O_2H_7N)_3(H_2O)_2](ClO_4)_3.H_2O$ at 4 K, show strong satellite bands which accompany the electron lines of $\Delta J = 0$, 2 (Figs. 2b and 3). They could be due to the vibronic coupling and a cooperative interaction; the latter one being facilitated by the short distance between the lanthanide ions in the dimeric unit of a polymer, created through carboxylic ridges. The high intensity of the vibronic lines is also a valuable proof of the comparatively high symmetry (D_2) of the metal ion. The analysis of the vibronic components has been carried out on the basis of the IR spectrum (Fig. 6) and Raman data. The vibronic components are promoted among others mainly by LnO_9 cluster modes and the internal ligand ν(COO) modes (Table 4), and have the highest intensities in accordance with the theory of vibronic transition probabilities [11–14].

The analysis of the cooperative components will be possible once diluted monocrystals are obtained.

4. Conclusion

1. X-ray analysis shows creation of endless polymeric chains composed of noncentrosymmetric dimeric subunits of two europium ions bridged by bidentate and

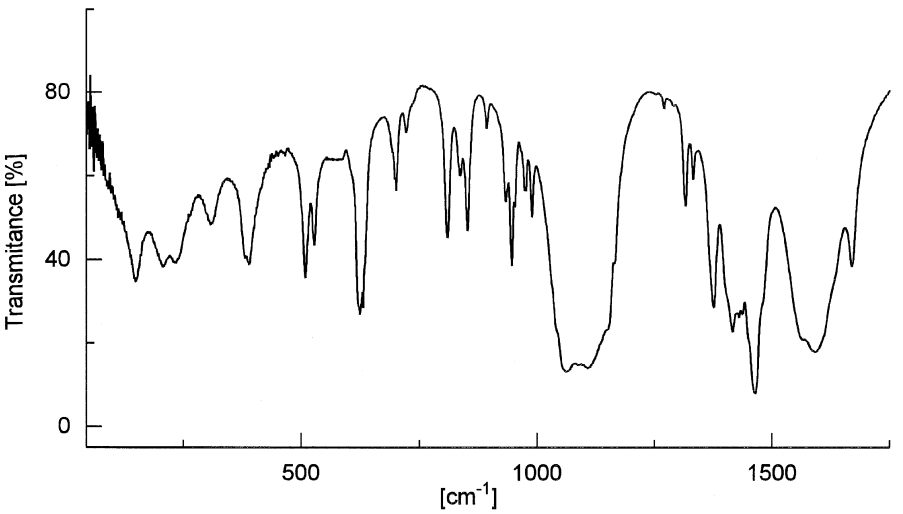

Fig. 6. IR spectrum of $[Eu(sar)_3(H_2O)_2](ClO_4)_3.H_2O$.

Table 4
Vibronic components of $[Eu(sar)_3(H_2O)_2](ClO_4)_3.H_2O$

Transition	Energy (cm^{-1})	ΔE (cm^{-1})	
$^5D_0 \rightarrow {}^7F_0$	17262		
	17160	102	τ(Ln–OCO–Ln)
	17102	160	
	17080	182	δ(LnO)
	17066	196	
$^5D_0 \rightarrow {}^7F_2$	16129		
	16014	115	δ(LnO)
	15964	165	
	15769	360	ν(COO)
	16211		
	16044	167	δ(LnO)
$^7F_0 \rightarrow {}^5D_2$	21464		
	21607	143	δ(LnO)
	21661	197	
	21716	252	ν(LnO)
	21743	279	

tridentate chelating carboxyl groups, which are further linked by two simple chelating carboxyl groups.
2. Europium ions occupy two symmetry positions with different M–L bonding lengths and CN 9.
3. Fitting of coordination polyhedra, performed by the Drew method, suggests intermediate TCTP and CSAP polyhedra are formed in the structure.
4. Analysis of the number of Stark components in high resolution emission and absorption spectra at 4 K allows us to determine the CF splitting and the D_2 symmetry of the metal center.
5. The intensity of the 0–0 transition is comparable with the vibronic components in the spectra.
6. The temperature dependence of the transition intensity is due to electron–phonon coupling, which is also manifested in relatively strong vibronic components, not only with internal ligand mode, but also to vibrations inside the MO_9 cluster.
7. The short M–M separation makes possible the cooperative interaction of coupled ions in the dimer. This needs, however, further confirmation in spectroscopic investigations of diluted single crystals.

Acknowledgements

The authors would like to thank Dr. P. Starynowicz for the X-ray fitting procedure of the coordination polyhedra of the title compound.

References

[1] W. Lenth, R.M. Macfarlance, Opt. Photonics News 3 (1992) 8, and references therein.
[2] F.S. Richardson, Chem. Rev. (1982) 541.
[3] W.D. Horrocks Jr., M. Albin, Prog. Inorg. Chem. 31 (1984) 1, and references therein.
[4] J. Legendziewicz, in: Excited States of Transition Elements, World Scientific, Singapore, 1998, p. 228.
[5] J. Legendziewicz, Acta Phys. Polonica 90 (1996) 127.
[6] M.P. Hehlen, U. Güdel, J. Chem. Phys. 98 (3) (1993).
[7] O. Khan, Molecular Magnetism, Verlag-Chemie, New York, 1993.
[8] C. Beneli, A. Caneschi, D. Gatteschi, L. Prodi, Mater. Chem. Phys. 31 (1992) 17.
[9] G. Oczko, J. Legendziewicz, J. Mrozinski, G. Meyer, J. Alloys Comp. 275 (1998) 219.
[10] K.M. Salikher, R.T. Galeev, V.K. Voronkova, Yu. Yablokov, J. Legendziewicz, Appl. Magn. Reson. 14 (1998) 457.
[11] C. de Mello Donego, A. Meijerniki, G. Blasse, J. Phys. Cond. Matter 4 (1992) 8889.
[12] G. Blasse, Int. Rev. Phys. Chem. 11 (1992) 71.
[13] A. Meijernik, C. de Mello Donego, A. Ellens, J. Systma, G. Blasse, J. Lumin. 58 (1994) 26.
[14] G. Blasse, A. Meijernik, C. de Mello Donego, J. Alloys Comp. 225 (1995) 24.
[15] J. Legendziewicz, E. Huskowska, Gy. Argay, A. Waskowska, Inorg. Chim. Acta 95 (1984) 57.
[16] T. Glowiak, C.N. Dao, J. Legendziwicz, E. Huskowska, Acta Cryst. C47 (1991) 78.
[17] T. Glowiak, J. Legendziewicz, E. Huskowska, P. Gawryszewska, Polyhedron 15 (1996) 2939.
[18] J. Legendziewicz, Z. Ciunik, P. Gawryszewska, J. Sokolnicki, Acta Phys. Pol. 84 (1993) 917.
[19] J. Legendziewicz, E. Huskowska, A. Waśkowska, Gy. Argay, Inorg. Chim. Acta 92 (1984) 151.
[20] J. Legendziewicz, E. Huskowska, Gy. Argay, A. Waśkowska, J. Less Common Metals 146 (1989) 33.
[21] J. Legendziewicz, P. Gawryszewska, E. Gałdecka, Z. Gałdecki, J. Lumin. 559 (1997) 72.
[22] J. Legendziewicz, P. Gawryszewska, A. Waskowska, Spectrochim. Acta A54 (1998) 2087.
[23] J. Legendziewicz, Z. Ciunik, P. Gawryszewska, J. Sokolnicki, Polyhedron 18 (1999) 2701.
[24] J. Legendziewicz, Acta Phys. Pol. 90 (1) (1996) 127.
[25] Kuma KM4 software, User's Guide, version 6.1, Kuma Diffraction, Wroclaw, Poland.
[26] N. Walker, D. Stuart, Acta Cryst. A39 (1983) 158.
[27] G.M. Sheldrick, Acta Cryst. A46 (1990) 467.
[28] G.M. Sheldrick, SHELXL97. Program for the Refinement of Crystal Structures, University of Göttingen, Germany, 1997.
[29] L.A. Asłanow, B.M. Ionow, I.D. Kiekraew, Coord. Chim. 2 12 (1976) 1674.
[30] M.G.B. Drew, Coord. Chem. Rev. 24 (1977) 179.
[31] G.S. Ofelt, J. Chem. Phys. 37 (1962) 511.
[32] B.R. Judd, Phys. Rev. 750 (1962) 127.
[33] J. Legendziewicz, K. Bukietyńska, G. Oczko, J. Inorg. Nucl. Chem. 43 (1981) 2393.
[34] A. Mondry, J.P. Riehl, Acta Phys. Pol. A 84 (1993) 969.